NASA TECHNICAL MEMORANDUM

NASA TM X-62,501

NASA TM X-62,501

COMPARATIVE STUDIES OF LUNAR, MARTIAN, AND MERCURIAN CRATERS AND PLAINS

V. R. Oberbeck and W. L. Quaide

Ames Research Center
Moffett Field, Calif. 94035

R. E. Arvidson

Washington University
St. Louis, Mo. 63130

H. R. Aggarwal

Santa Clara University
Santa Clara, Calif. 95050

September 1975

1. Report No.	2. Government Accession No.	3. Recipient's Catalog No.
NASA TM X-62,501		

4. Title and Subtitle	5. Report Date
COMPARATIVE STUDIES OF LUNAR, MARTIAN, AND MERCURIAN CRATERS AND PLAINS	6. Performing Organization Code

7. Author(s)	8. Performing Organization Report No.
V. R. Oberbeck,* W. L. Quaide,* R. E. Arvidson,** and H. R. Aggarwal†	A-6339

9. Performing Organization Name and Address	10. Work Unit No.
*Ames Research Center, Moffett Field, Calif. 94035 **Washington University, St. Louis, Mo. 63130 †Santa Clara University, Santa Clara, Calif. 95050	384-50-60-02
	11. Contract or Grant No.
	13. Type of Report and Period Covered Technical Memorandum
12. Sponsoring Agency Name and Address National Aeronautics and Space Administration Washington, D. C. 20546	14. Sponsoring Agency Code

15. Supplementary Notes

Presented at the International Colloquium of Planetary Geology, Rome, Italy, 22–30 September 1975.

16. Abstract

The spatial distribution of lunar smooth plains is not consistent with experimental simulations of melt rock emplacement during cratering in layered materials. Nor is it consistent with the location of melt rocks (suevite) near the Ries basin. Lunar smooth plains surrounding Imbrium are most extensive in areas where pre-existing craters are most degraded. This observation suggests that plains form by impact of basin and local primary crater ejecta, together with deposition of debris excavated by the resultant secondary cratering events. Craters within the belt of smooth plains surrounding the Caloris basin on Mercury are most degraded nearest the basin. This suggests that Mercurian smooth plains must, at least in part, be emplaced in a manner similar to plains surrounding the Imbrium basin.

Mercurian uplands have a primary crater population deficient in small crater diameters ($\lesssim$ 30 km). Lunar uplands far from major basins also have a crater population deficient in small crater sizes. We suggest that the lunar uplands have a primary crater population deficient in crater sizes $\lesssim$30 km. However, the deficiency has been masked in most areas by numerous secondary craters formed by impact of ejecta from major basins. Martian cratered terrain exhibits a similar crater deficiency, which has previously been interpreted as due to obliteration of small craters ($\lesssim$ 30 km) by some surface process. We suggest that most of the smaller craters on Martian uplands were never produced and that surface processes were only responsible for obliteration of secondaries ($\lesssim$ 10 km) produced by the larger ($\gtrsim$ 30 km) primary craters.

A crater size distribution deficient in small sizes ($\lesssim$ 30 km) on the Mercurian, lunar, and Martian uplands has implications for the origin of debris bombarding the inner solar system during the period recorded by these surfaces. We propose that during late heavy bombardment, the inner solar system was inundated with bodies that broke up under tidal fission as they approached the planets. Such a mechanism would lend to production of a crater population deficient in small crater sizes and it would also explain the large degree of spatial clustering of primary craters on Mercury, the moon, and Mars.

17. Key Words (Suggested by Author(s))	18. Distribution Statement
Comparative photogeology Lunar Martian and Mercurian Intercrater plains Smooth plains	Unlimited STAR Category – 42

19. Security Classif. (of this report)	20. Security Classif. (of this page)	21. No. of Pages	22. Price*
Unclassified	Unclassified	35	$3.75

*For sale by the National Technical Information Service, Springfield, Virginia 22151

COMPARATIVE STUDIES OF LUNAR, MARTIAN, AND MERCURIAN CRATERS AND PLAINS

V. R. Oberbeck,* W. L. Quaide,* R. E. Arvidson,** and H. R. Aggarwal†

1. Introduction

Comparative photogeology of Mars, Mercury, and the moon is imperative now that comparable imagery data exists. Studies of Martian, Mercurian, and lunar imagery supplement one another since variations in planetary conditions can provide checks on hypotheses developed to explain features or processes on only one surface. In addition, past lunar work can provide clues to explain grossly similar features observed on other planetary surfaces. In this paper, we take a comparative approach to treating the problems of: (1) the origin of lunar and Mercurian smooth plains, (2) explanations for the relative degradation states of craters on Martian, Mercurian, and lunar uplands, and (3) reasons for the deficiency of craters $\lesssim$ 30 km in diameter on Martian, Mercurian, and lunar uplands, and for the non-random spatial distribution of craters on these surfaces.

2. Lunar Smooth Plains

Lunar smooth plains have been mapped as Imbrian in age on the geologic map of the front surface of the moon (Wilhelms & McCauley, 1971). They are restricted to uplands terrain, where they are found both inside craters and between craters. Figure 1 shows their distribution. The largest patches are located near the Imbrium basin. If present beneath maria lava flows they form a belt concentric to Imbrium. Most smooth plains are very flat and the surface is typically covered by subdued craters (Eggleton & Schaber, 1972). Prior to the Apollo missions most investigators suggested that plains were volcanic in origin. However, samples

---

*Ames Research Center, Moffett Field, Calif.

**Washington University, St. Louis, Mo.

†Santa Clara University, Santa Clara, Calif.

collected from smooth plains at Descartes (Apollo 16) are dominantly impact breccias, suggesting an impact origin for smooth plains (LSPET, 1973). Considerable disagreement exists as to the mode of smooth plains emplacement. The possibility that plains might be impact melts has been advanced (Howard & Wilshire, 1974). Another possibility is that smooth plains consist of Orientale ejecta (Moore et. al., 1974). Another hypothesis is that smooth plains material consists of ejecta from basins and local primary craters, together with material excavated from secondary craters associated with the basin and local crater-forming events (Oberbeck et. al., 1973, 1974; Oberbeck, 1975; Head, 1975).

We now demonstrate that the last-mentioned hypothesis must be considered a viable mechanism for plains formation. Figure 2 is a schematic illustration of ejecta positions derived from an analytical model for the Copernicus cratering event (Oberbeck, 1975). Calculated launch angles and velocities for material ejected from Copernicus (Shoemaker, 1962) are used as initial input to the model. Ejecta is found at any given time after ejection, but before impact, in an inverted conical sheet. Material launched from near-surface material earliest in the cratering process is ejected at highest velocities. It is found at any given time at the highest positions in the expanding sheet. Later, material is launched at lower velocities from a hemispherical shell that contains both the near surface material and material at depth. This ejecta is found at any given time at the lowest positions in the sheet. Material impacts outside the crater rim from the base of the sheet. Progressively higher impact velocities occur as the sheet expands. For large events (Copernicus, basin-sized events), velocities of impacting fragments are high enough, even within the vicinity of the continuous deposits, to

produce cratering and mixing of pre-existing materials. In the schematic, we show this mixture of material moving radially behind the conical sheet because it must have a lower velocity than the impacting material. The indicated sequence for emplacement of deposits at any given range beyond about 2 km from a large crater is: (a) extensive erosion of pre-existing materials by impact of crater ejecta, and (b) blanketing by a radial surge which is a mixture of basin and secondary crater ejecta. Material contained within the surge is likely to be ponded in depressions, such as pre-existing craters, that may surround the primary crater.

Morrison and Oberbeck (1975) have suggested that the morphology of ejecta deposits surrounding the lunar crater Linne (2 km in diameter) can best be explained by secondary cratering followed in time by a radially expanding debris surge. The topography of Linne's ejecta deposits consists of dune-like forms concentric to and near the crater rim. Further away from the rim, but still on the continuous deposit, concentric dune-forms are paired with concentric crater chains. At positions outside the continuous deposits, only concentric chains occur. The concentric crater chains are best explained by impact of loops of closely spaced fragments at the base of the Linne ejecta curtain. The dunes close to the crater and the dunes associated with crater chains are also related to formation of closely spaced secondaries. Collision between ejecta rrom these craters and the advancing debris surge would cause piling-up of material on the uprange rims of the crater chains, resulting in concentrically arranged dunes. Similar dune-like features have also been observed around Martian craters (Arvidson et al. 1975). We believe the Linne crater observations verify the essential components of our ejecta emplacement

model even for very small lunar craters.

During emplacement of ejecta from basins, extensive erosion by secondary cratering and a massive subsequent radial debris surge may be capable of producing smooth plains deposits that are a mixture of local material and basin material. Observational evidence of these effects may be the presence of lineated terrain cutting the walls of Ptolemaeus crater, and the large expanse of plains (products of debris surge) which later filled the floor of Ptolemaeus. Figure 3 shows that there are well developed grooves in the rim of Ptolemaeus, but only remnants of grooves on the crater floor, We believe that the grooves on the walls and the floor were produced by the passage and basal cratering of the inclined conical curtain of Imbrium ejecta. Later the debris surge passed over the region, debris ponded on the crater floor, and the grooves on the crater floor were nearly obliterated.

The observations and interpretations of Ptolemaeus suggest that there should be a direct relationship between the extent of lineated terrain and plains, and the degree of degradation of pre-existing craters. Further evidence can be derived from Figure 4, which is a portion of the lunar nearside geologic map, overlain with contours representing areal densities of Ronca and Green's (1970) degraded craters. Specifically, the contours represent the percentage of their class 4 and 5 craters. Ronca and Green (1970) used the data compiled in the Arthur Catalogs ; Class 4 and 5 craters represent ghost craters and craters with ruined walls. Inspection of Figure 4 shows that the highest percentage of these craters exists near Ptolemaeus, where there are the greatest amounts of lineated terrain, and also the largest areal extent of plains. Moving to the southeast, progressively less area

is covered by plains; lower percentages of old degraded craters are also encountered. Ronca and Green (1970) noted that highest fresher crater concentrations occur well inside terra boundaries. They explained this pattern as due to effects of basin formation. We agree, and suggest the effect is due to basin secondaries and ejecta of secondaries (debris surge) that more extensively degraded and obliterated pre-existing craters near the maria-terra boundaries; the debris surges ponded in the floors of many craters and buried more of the small craters on the margins of the terra than in the central terra. This would explain why degraded craters and plains materials are nearer to basin margins. It would also explain the nesting effect of greatest number of surviving pre-existing craters in the central southeastern highlands, as described by Ronca and Green (1970).

3. Mercurian smooth plains

Strom et al. (1975) suggest that Mercurian smooth plains are volcanic in origin. The main arguments for volcanic origin are that the smooth plains cover too large an areal extent to be explained either as an impact melt phenomena or as a mixture of local material and basin ejecta. Also, presence of plains inside basins, and differences of color of plains internal and external to basins, is cited as evidence of non-impact origin of plains.

Wilhelms (1975) notes that suggestions of a volcanic origin of Mercurian plains are similar to earlier suggestions of volcanic origins for lunar smooth plains. We now explore the possibility that Mercurian plains may in fact have formed in a manner analogous to formation of lunar smooth

plains — by ballistic erosion and sedimentation. Figure 5 shows a large crater to the northeast of the Caloris basin. Reference to the geologic map of Trask and Guest (1975) shows that terrain west of this crater is mapped as lineated terrain and the crater floor contains smooth plains. The pattern of disected walls and the plains associated with this crater are similar to that observed in Ptolemaeus (Figure 3). The lineated terrain on the crater rim was probably produced by secondary cratering caused by impact of Caloris ejecta. By analogy with Ptolemaeus, at least some fraction of the smooth plains on the crater floor must have been emplaced during the Caloris event.

There is compelling additional evidence that other smooth plains concentric to Caloris are also, at least in part, mixtures of pre-existing material and Caloris ejecta. We have classified craters found between the rim of Caloris and the limit of the continuous belt of smooth plains peripheral to Caloris, using a modified method of crater classification after Arvidson (1974). Figure 6 illustrates the classification. Class 1 craters are fresh with sharp crater rims, they typically have terraces, central peaks or both. Class 2 craters are degraded in appearance: they lacking distinctly raised rims; terraces and central peaks are degraded or absent. Class 3 craters are highly modified by lineations cutting across their walls; they are usually very shallow and rimless. We classified each of the craters in the continuous smooth plains surrounding Caloris basin that have been mapped by Trask and Guest (1975) as having smooth plains. Figure 7 shows results of the classification, together with crater rim and floor diameters and distances of crater centers from

the center of the Caloris basin. Class 3 craters, which are the most degraded, are nearest the basin and are filled most with plains (D crater/ D plains all nearest 1). The proportion of plains filling craters decreases as the distance from Caloris increases and, coincident with this change, is the gradual increase of the number of class 2 craters and then at greater ranges, class 1 craters. Within the continuous belt of plains surrounding Caloris, the most eroded craters contain the greatest amount of plains and they are present nearest the rim of Caloris. The increase in crater degradation and amount of plains near the basin is similar to that found for craters and plains surrounding the lunar Imbrium basin (Figure 1). Massive crater modification by secondary cratering must have been associated with the Caloris event. By analogy with the moon, massive amounts of smooth plains may have formed as the associated debris surge spread radially away from Caloris and ponded in topographic lows. At least some fraction of these Mercurian smooth plains must therefore be related to ballistic erosion and sedimentation associated with secondary cratering.

The geologic map of Trask and Guest (1975) shows that Mercurian smooth plains associated with Caloris and external to it are much nearer and much more continuous than is the distribution of plains surrounding lunar basins. Such differences are consistent with our mechanism of formation. Figure 2 shows our model of secondary ejecta impact, cratering, and formation of a debris surge. Projectiles impacting with identical masses and velocities on Mercury and the moon will eject fragments that have the same mass-velocity distributions. Range of a given mass of ejected material is a function of ejection angle, launch velocity, and the gravitational acceleration.

The range of basin ejecta launched at similar velocities and angles will therefore be less on Mercury than on the moon, because of higher Mercurian gravity. The debris surge that occurs after passage and impact of basin ejecta also will be more confined on Mercury than on the moon because of high gravity. The relative confinement of plains near Caloris is thus qualitatively consistant with our model of emplacement. Gault et. al. (1975) have used similar but simpler arguments based only on transport of primary crater ejecta to explain the closer appearance of secondary craters around Mercurian Primary craters.

There is additional evidence that basin ejecta impacts closer to basins on Mercury than on the moon. Strom et al. (1975) have noted an absence of a radial facies in the deposits surrounding Caloris; instead there are sets of ridges and depressions concentric to the Caloris basin rim at ranges where the radial facies is observed in deposits of the similar-sized lunar Imbrium basin. Figure 8 shows a photograph that best illustrates these ridges. Morrison and Oberbeck (1975) have shown that radial facies surrounding the Imbrium basin is probably due to collision of ejecta from separated radial chains of basin secondaries. On Mercury, relatively more ejecta must have impacted at ranges now occupied by lunar radial facies. We hypothesize that the density of impacting ejecta was high enough on Mercury that no separated radial crater chains occurred at these ranges. If so, we should expect features similar to those that appear much nearer lunar craters and basins. Morrison and Oberbeck (1975) illustrated concentric dunes paired with secondary craters near the rims of lunar craters that show gross similarity to the pattern of ridges illustrated in Figure8 . This suggests that the concentric ridge and

depression facies described by Strom et al.(1975)might be due to secondary impact processes.

4. Smooth Plains as Impact Melts

Certain observations of impact melts surrounding the Ries crater in Germany are relevant to testing the hypothesis that lunar and Mercurian plains are melt rocks. The Ries crater formed in sedimentary rock layers (~ 1 km total thickness) overlying crystalline bedrock. Melt rock material known as suevite lies unconformably on the bulk ejecta of the Ries, which is a mixture of local materials and material ejected from the Ries crater. Most of the melt products are found between the crater rim and one crater radius away from the rim. In this regard it is similar to the distribution of candidate melts around lunar craters, the positions of which have been reported by Howard and Wilshire (1974). Ries melts may be valid analogs for these lunar deposits. However, they are not good analogs for lunar smooth plains, which are more abundant and are found at much greater relative ranges from the rims of lunar basins. If lunar smooth plains are melt deposits, a major change in melt emplacement for only basin-sized events is required. Without a plausible explanation for such a major change, the case for melt origin of plains is weakened.

Discussion of melt rocks raises the nagging question of why they are found stratigraphically above all other ejecta. We have simulated target materials at the Ries crater and have performed laboratory impact tests in an attempt to answer this question. The ratio of the thickness of the low strength, low density sedimentary rocks to the size of the crater is about 1:20. In our laboratory impact experiment, a thin layer of blue quartz sand was placed above an high strength white sandstone (pro-

duced by bonding quartz with epoxy resin), in ratios suitable for simulation of the Ries target geometry. Plastic lexan projectiles were fired into the target with a velocity = 6.0 km/sec. The result was formation of a small crater in the substrate material and a large outer crater in the weak surficial sand target material. The Ries crater has a similar geometry. The white substrate material was deposited on top of the blue surface material, in a process that we think is similar to emplacement of suevite (crystalline basement material) on top of the Ries crater bunte breccia deposits (Figure 9). Examination of the high speed motion pictures of the laboratory impact simulation demonstrates that blue surface material was ejected at low angles to form the conical sheet, but that substrate material was ejected simultaneously at near vertical angles (Figure 10). Because of longer flight times, the near-vertical ejecta impacted after deposition of low-angle ejecta. Near-vertical trajectories kept the material close to the crater rim.

Since near-surface layering exists on the moon, our laboratory simulations may provide an explanation for why melt rocks are close to primary crater rims. Major crustal discontinuities may also be present on the moon. Multi-ringed structures in basins conceivably form by shock-wave reflections from major seismic discontinuities. In fact, the Ries crater exhibits multiple rings that are thought to form by cratering in seismically inhomogeneous material (Johnston et al. 1964). If the lunar basins penetrated crustal discontinuities then melts would be found near the basin rims and not at the positions of smooth plains. If no curstal inhomogeneities were present then melts should have been widely dispersed at high velocity. Most likely, upon impact, melt material would produce cratering and mixing with pre-existing material. Large, continuous ponds of melt would probably not form

at great distances from basins. Thus, we do not believe that lunar smooth plains can be exclusively basin impact melts.

If crustal discontinuities exist on Mercury then the smooth plains surrounding Caloris may have some component of origin related to melt emplacement. However, we note that high-energy ejecta would also impact closer to Caloris (higher Mercurian gravity), leading to enhanced secondary cratering and thus probably plains formation at relatively short ranges.

5. Deficiency of Small Bodies in the Late Heavy Bombardment of the Inner Solar System

Trask and Guest (1975) have divided Mercurian uplands into two units: heavily cratered terrain and intercrater plains. Intercrater plains are considered to be the older of the two, since plains cannot be seen to overlap onto crater deposits. Also, the small, irregular secondary craters that cover intercrater plains seem to have originated from craters on heavily cratered terrain. Murray et. al. (1975) suggest that this evidence means that Mercury was completely re-surfaced, probably by volcanism, very early in its history. Heavily cratered terrain must then represent some subsequent impact record, perhaps the record of late heavy bombardment. The implication is that this bombardment phase on Mercury was deficient in small bodies since Mercurian uplands show a marked deficiency of craters $\lesssim$ 30 km in diameter.

Trask and Guest (1975) provided the clue necessary to demonstrate a similar global deficiency of lunar primaries less than 30 km in diameter. They noted that only small parts of the lunar surface resemble Mercurian uplands, i.e. only small parts are markedly deficient in smaller crater

sizes. In Figure 11 we show the lunar area suggested by Trask and Guest (1975) to be analogous to Mercurian uplands, together with another area to the north that appears more typically lunar. We have also plotted on the figure contours of combined ejecta from lunar basins (Short & Foreman, 1972), and also the irregular chained and clustered craters ($\lesssim$ 40 km) mapped by Wilhelms and McCauley (1971). The contour lines of Short and Foreman represent only the thickness of ejecta that would have resulted if ejecta did not crater the surface. We interpret the contours to reflect a relative measure of the mass of impacting material that would produce secondary craters. Note that the area that resembles Mercurian terrain lies in a region least influenced by basin ejecta; it is also deficient in irregular clustered and chained craters ($\lesssim$ 40 km) which are present in most other regions. This raises the possibility that the irregular chained and clustered craters are secondaries and that most lunar areas reveal no deficiency in primary craters $\lesssim$ 30 km (like Mars and Mercury) because of relatively widespread distribution of secondaries. However, the deficiency is readily apparent on Mercury where basin secondaries are, because of the higher gravity field, not widely distributed. The deficiency may also be more apparent because of a dearth of basins on Mercury as opposed to the moon.

Obscurity of the deficiency of small primary craters by abundant lunar basin secondaries can be graphically illustrated from consideration of the typically lunar area in Figure 11. We believe this area, which is north of the area illustrated by Trask and Guest (1975), appears lunar-like because it has large numbers of irregular, chained and clustered craters ($\lesssim$ 40 km) as mapped by Wilhelms and McCauley (1971). Wilhelms and McCauley

favored a volcanic origin for these craters, but their alternate hypothesis was that they were secondary craters. In either case, they should not be considered in deriving the primary flux. This area can be made to appear Mercurian if we remove only the irregular chained and clustered craters less than 40 km from the scene. Even if they are volcanic craters they do not reflect the primary flux and should be removed. In figure 12 we present both the original view of Figure 11, with the irregular chained and clustered craters, and a view derived by airbrush removal of the chained and clustered craters. The modified view shows a much closer resemblance to Mercurian uplands. In sum, we suggest that the lunar uplands were also bombarded by a population deficient in small bodies. We propose that the deficiency was obscured mainly by innumerable large secondary craters formed by impact of basin ejecta.

We have discovered a septa and herringbone ridge element diagnostic of known lunar secondary craters (Oberbeck & Morrison, 1974) on the 30 km crater Horrocks located on the floor of Hipparchus crater. Figure 13 shows a photograph that reveals a small crater east of Horrocks that is joined to Horrocks by straight wall (septum). A V-shaped herringbone ridge projects from the septum. These features have been produced in the laboratory by simultaneous formation of closely-spaced impact craters. Horrocks is an irregular compound crater having all the characteristics of much smaller, well documented lunar secondary craters. This observation provides additional evidence that secondary craters can be as large as 30 km and therefore that the irregular clustered and chain craters mapped by Wilhelms and McCauley (1971) are basin secondaries.

We believe the deficiency in small bodies during bombardment of the moon and Mercury also existed during late bombardment of Mars. Figure 14

shows similar-sized scenes of cratered terrain on the moon, Mars, and Mercury. A scene containing irregular chained and clustered craters $\lesssim$ 40 km on the moon is also shown on the lower right corner. However, assume, based on the past arguments, that the lunar scene in the upper right hand corner best reflects the true primary flux during the late bombardment, even though this type terrain is rare on the moon. We can then understand why this lunar scene is so similar in appearance to the Mercurian scene, if we acknowledge that both scenes were unaffected by large basin secondaries. We now note that Martian heavily cratered terrain is similar to both Mercurian terrain and the lunar scene because all lack smaller ($\lesssim$ 30 km) craters.

6. Degradation of craters and formation of plains in craters distant from basins

A major problem in comparative planetology is the unraveling of processes responsible for degradation of Mercurian, lunar and Martian craters in uplands terrain. Comparison of the size-frequency distribution of craters in Martian and lunar uplands led to the observation of a deficiency of craters $\lesssim$ 30 km on Mars. This observation, combined with the degraded appearance of flat-floored Martian craters and the relatively featureless appearance of Martian intercrater terrain, led to hypotheses invoking some previous episode of large-scale obliteration of Martian surface features (Opik, 1966; Murray et al. 1971; Hartmann, 1973; Chapman, 1974; Jones, 1974). However, as discussed, comparison of lunar, Martian, and Mercurian uplands leads to a different hypothesis. Many of the supposedly obliterated smaller ($\lesssim$ 30 km) craters on Mars were never produced. Intercrater

plains similar to Mercurian plains have in fact been mapped on Mars (Wilhelms, 1974). Degradation processes on Mars need only to have obliterated many of the small secondary craters like those superimposed on Mercurian intercrater plains.

Soderblom et. al. (1974) suggest that degradation of large ($>$ 15 km) craters on Martian uplands occurred concurrent with heavy bombardment. Chapman (1974) and Jones (1974) independently suggested that uplands crater morphologies demonstrate some episode (wind, water, etc.) of obliteration that occurred after heavy bombardment ceased. They used the crater classification developed by Arvidson(1974), which, unfortunately, suffers from relatively large errors in classifying craters (due to resolution-limits) just at the crater diameters at which their arguements are crucial. Until Mariner 9 narrow-angle frames are analyzed, we choose to accept the first hypothesis: crater degradation is linked to cratering rate.

One degradation mechanism that could have been operative during heavy bombardment is enhanced secondary cratering due to the presence of non-impact-produced regolith. However, as discussed above, the total amount of crater degradation and obliteration has probably been much less than previously thought. Oberbeck et al. (1974) derived an expression for the ratio of the total mass ejected by all secondaries of a given primary (M_{sc}) to the mass ejected from the primary (M_{pt}). This depends on μ, which for any given secondary crater is the ratio of ejected mass to projectile mass. μ is an inverse function of secondary crater size. If secondaries from a given-sized primary on Mars were characteristically smaller than on the moon, then relatively more mass would have been redistributed for a given event on Mars.

Arvidson and Coradini(1975) showed that crater diameter-frequency distributions for craters superimposed on Martian fretted terrain demonstrate that much of fretted terrain probably formed concurrent with and immediately after last stages of heavy bombardment. A considerable amount of fine-grained debris must have been produced during the fretting process. If this debris were spread over uplands terrain as a blanket, then a non-impact regolith would have been penetrated by subsequent uplands impacts. Compared to Mercury or the moon, a relatively large fraction of fine-grained material would have been ejected and numerous small secondary craters would have formed. The result may have been an enhanced degration rate (relative to the moon) for a given cratering rate.

7. Late Heavy Bombardment in the Inner Solar System

We have presented evidence that there was a deficiency in small bodies required to form primary craters smaller than~30 km during the late heavy bombardment of the moon, Mars, and Mercury. We now discuss whether this evidence, combined with morphologic and statistical data for crater populations, can yield clues as to the process that produced bodies during the late bombardment of lunar and planetary surfaces in the inner solar system.

Oberbeck and Aoyagi (1972) have noted that the spatial distribution of craters in Martian heavily cratered terrain is non-random. They adopted the calculations of Sekiguichi (1971) to explain clustering of craters on the Martian surface as being due to tidal distruption of weak meteoroids and comets in the vicinity of Mars. Trask and Guest (1975) note that Mercurian heavily cratered terrain also contains clusters of craters. Finally, crater clustering has also been observed on the lunar uplands (Elston et al. 1971). Apparently, clustering of primary craters, in

addition to deficiency of small crater sizes, was a common feature of heavy bombardment. Chapman (1974) argues that the observed clustering on Mars is apparent and due to preferential removal of $\lesssim$ 30 km craters, although he never explicitly states how obliteration can lead to clustering. Aggarwal and Oberbeck (1975), using only craters > 30 km, demonstrated a marked non-random clustering over the entire equatorial Martian uplands.

Such constraints as to size and clustering may be best met by processes of tidal disruption of larger impacting bodies. Tidal disruption occurs under low stress levels, unlike asteroid-asteroid collisional processes (Aggarwal & Oberbeck, 1974; Dohnanyi, 1972). Very high stresses during impact result in large numbers of small fragments (Gault & Wedekind, 1969; Opik, 1971). On the other hand, tidal break-up should result in a relative deficiency of small bodies.

Wetherill (1975) has argued that it is necessary to conceive of some process that can allow for a late bombardment hundreds of millions of years after the accretionary phase of bombardment. He offers convincing arguements that Roche limit breakups were probable and that perturbations in orbits of products of tidal disruption of a very large body would take long enough to provide for a late heavy bombardment in the inner solar system. He has demonstrated that the impact flux that would result from this process would be about the same throughout the inner solar system. We point out that clustering, deficiency of small bodies, and similarity in the primary crater frequency of the 3 surfaces of Figure 14 is consistent with Wetherill's (1975) mechanism for production of the fragments for late bombardment.

Acknowledgements

Research reported in this paper was supported by the planetology programs office of the office of space sciences, NASA headquarters. Thanks are extended to the national space science data center for prompt delivery of imagery.

References Cited

Aggarwal, H.A., and V.R., Roche Limit of a Solid Body, The Astrophysical Journal, 191,577-588, 1974.

Arvidson, R.E., Morphologic classification of Martian craters and some implications, Icarus, 22, 264-271, 1974.

Arvidson, R.E., and M. Coradini, Crater diameter-frequency distributions for Martian Fretted terrain, International Colloquim of Planetary Geology, Rome, Sept., 1975.

Arvidson, R.E., M. Coradini, A. Carusi, A. Coradini, M. Fulchignoni, C. Federico, R. Funiciello, and M. Salomone, Latitudinal variation of wind erosion of crater ejecta deposits on Mars, Icarus, in press.

Chapman, C.R., Cratering on Mars, II, Cratering and Obliteration History, Icarus, 22, 272-291, 1971.

Dohnanyi, J.S., Interplanetary objects in review: Statistics of their masses and dynamics, Icarus, 17, 1-48, 1972.

Eggleton, R.E., and G.G. Schaber, Cayley Formation interrelated as basin ejecta, Apollo 16 Preliminary Science Report, NASA SP 315, Part 29-7, 1972.

Elston, W., M. Aldrich, E. Smith, and R. Rhodes, Nonrandom distribution of lunar craters, Journal of Geophys. Res., 76, 5675-5682, 1971.

Gault, D.E., and J. Wededind, The destruction of tektites by micrometeoroid impact. Journal of Geophys. Res., 74, 6780-6794, 1969.

Hartmann, W.K., Martian cratering, 4, Mariner 9 initial analysis of cratering chronology, Journal of Geophys. Res., 78, 4096-4116, 1973.

Head, J.W., Processes of Lunar crater degradation: Changes in style with geologic time, The Moon, 12, 299-329, 1975.

Howard, K.A., and H.G. Wilshire, Flows of impact melts at Lunar craters, Journal of Res. U.S. Geol. Surv., 1975.

Jones, K.J., Evidence for an episode of crater obliteration intermediate in Martian history, Journal of Geophys. Res., 79, 3917-3932, 1974.

LSPET (Lunar Sample Preliminary Examination Team), Science, 179, 23-24, 1973.

Moore, H.J., C.A. Hodges, and D.H. Scott, Multiringed basins illustrated by Orientale and associated features, Proc. Lunar. Sci. Conf. 5th., 1, 71-100, 1974.

Morrison, R.H., and V.R. Oberbeck, Geomorphology of crater and basin deposits - Emplacement of the Fra Mauro Formation, Proc. 6th Lunar Sci. Conf., Pargamon Press Geochem. Et. Cosmochim (in Press), 1975

Murray, B., L. Soderblom, R. Sharp, and J. Cutts, The surface of Mars: 1. Cratered terrains, Journal of Geophys. Res., 76, 313-330, 1971.

Murray, B.C., R.G. Strom, J.J. Trask, and D.E. Gault, Surface history of Mercury: Implications for terrestrial planets, Journal of Geophys. Res., 80, 2508-2514, 1975.

Oberbeck, V.R., and M. Aoyagi, Martian doublet craters, Journal of Geophys. Res., 77, 2419-2432, 1972.

Oberbeck, V.R., F. Horz, R.H. Morrison, and W.L. Quaide, Emplacement of the Cayle Formation, NASA TMX 62-302, 1973.

Oberbeck, V.R., and R.H. Morrison, Laboratory simulations of the herringbone pattern, associated with Lunar secondary crater chains, The Moon, 9, 415-455, 1974.

Opik, E.J., The Martian surface, Science, 153, 255-265, 1966.

Opik, E.J., Cratering and the Moon's surface, in Advances in Astronomy and Astrophysics, Vol. 8, ed. by Z. Kopal, 108-337, Academic, N.Y. 1971

Ronca, R.B., and R.R. Green, Statistical geomorphology of the Lunar surface, Geol. Soc. Amer. Bull., 81, 337-352, 1970.

Sekiguchi, N., On the fissions of a solid body under influence of tidal force, with application to the problem of twin craters on the Moon, The Moon, 1, 429, 1970.

Shoemaker, E.M., Interpretation of Lunar craters, in Physics and Astronomy of the Moon, Z. Kopal Ed., Academic Press, N.Y. 538, 1962.

Short, N.M., and M.L. Forman, Thickness of impact crater ejecta on the Lunar surface, Mod. Geol., 3, 69-91, 1972.

Strom, R.G., N.J. Trask, and J.E. Guest, Tectonism and volcanism on Mercury, Journal of Geophys, Res., 80, 2478-2507, 1975.

Trask, N.J., and J.E. Guest, Preliminary geologic terrain map of Mercury, Journal of Geophys. Res., 80, 2461-2477, 1975

Wetherill, G.W., Late heavy bombardment of the Moon and terrestrial planets, Proc. of the 6th Lunar Sci. Conf., Pargamon Press, (in press), 1975.

Wilhelms, D.E., Mercurian volcanism doubted, International Planetary Colloquim, Pasadena, Ca., June 25-27, 1975.

Wilhelms, D.E., and J.F. McCauley, Geologic map of the near side of the Moon, U.S. Geol. Surv. Misc. Geol. Inv. Map I 703, 1971.

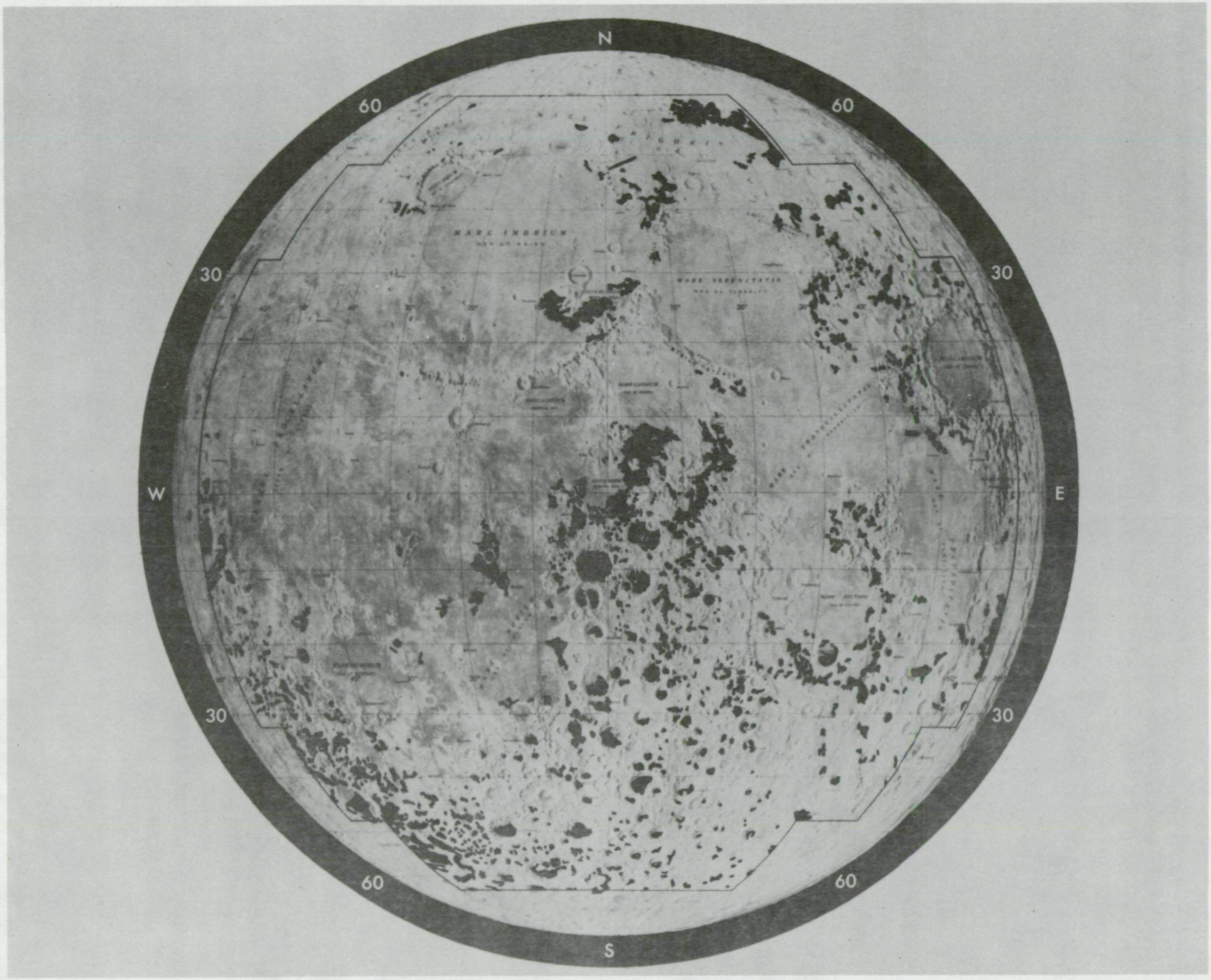

Figure 1.- Distribution of lunar smooth plains, which are shown in black.

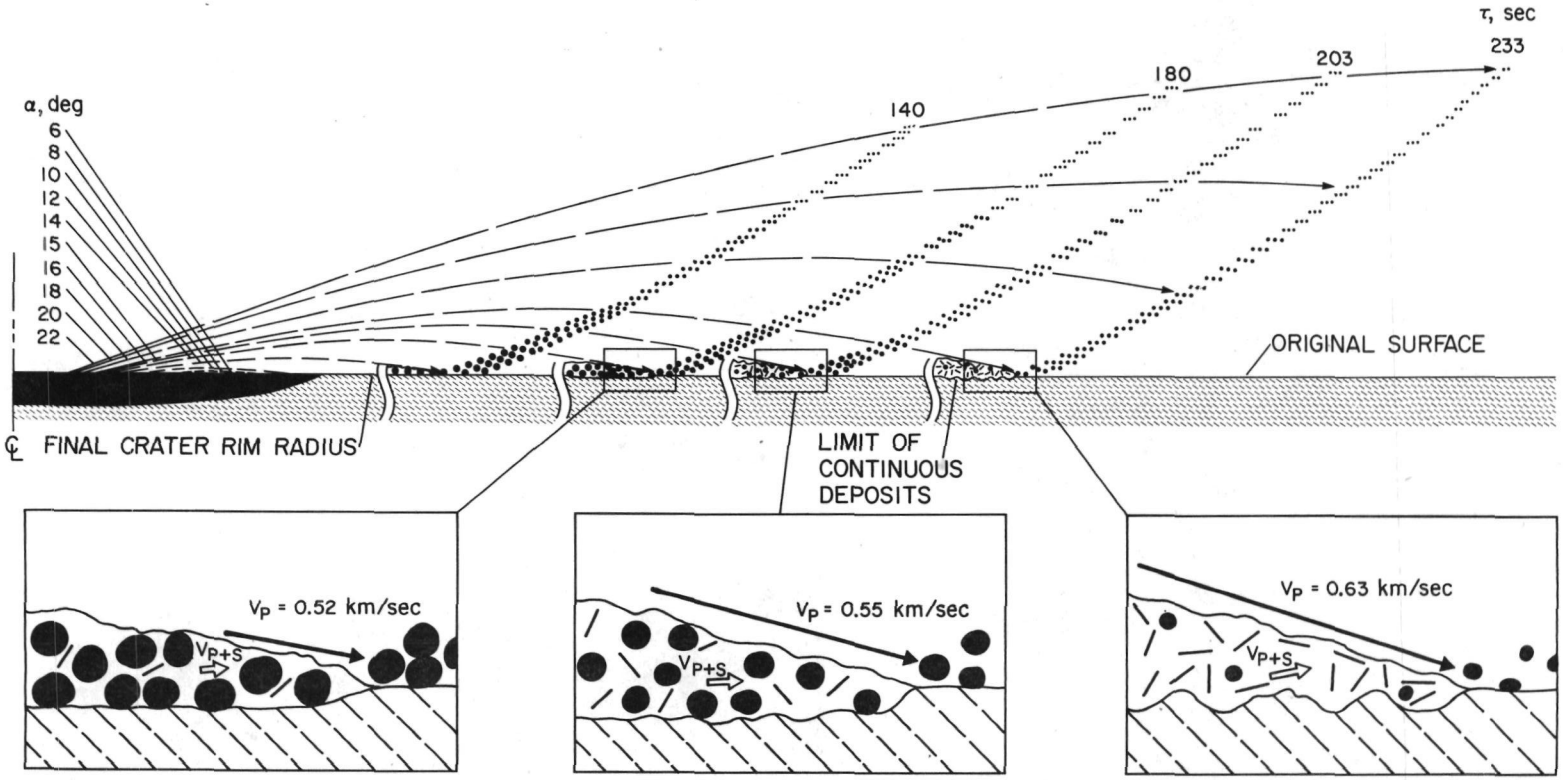

Figure 2.- Schematic illustration of the relative positions of ejecta at various times, T, after excavation. V_p refers to impacting velocity of the projectiles, while V_{p+s} indicates a low velocity mixture of primary and secondary debris.

Figure 3.- Lunar crater Ptolemaeous showing the linear sculpturing on the crater rim and walls. Note the remnants of sculpturing on the crater floor beneath the smooth plains.

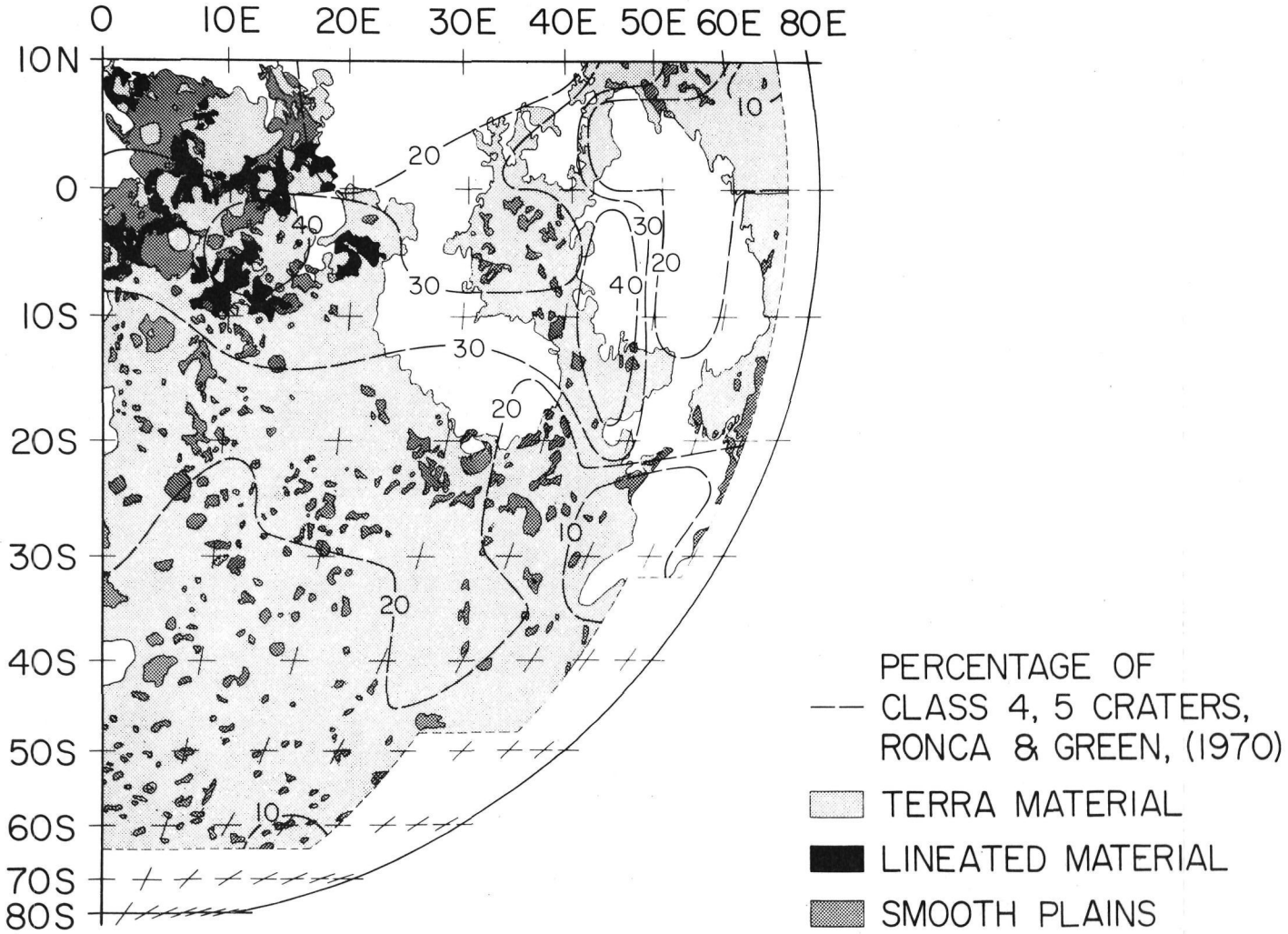

Figure 4.- Contours of percentages of class 4 and 5 craters from Ronca and Green (1970) and distribution of lunar lineated terrain and smooth plains.

Figure 5.- Crater to the northeast of the Mercurian Caloris basin. Note that the walls and rim are cut by lineated terrain and that the floor is covered by smooth plains.

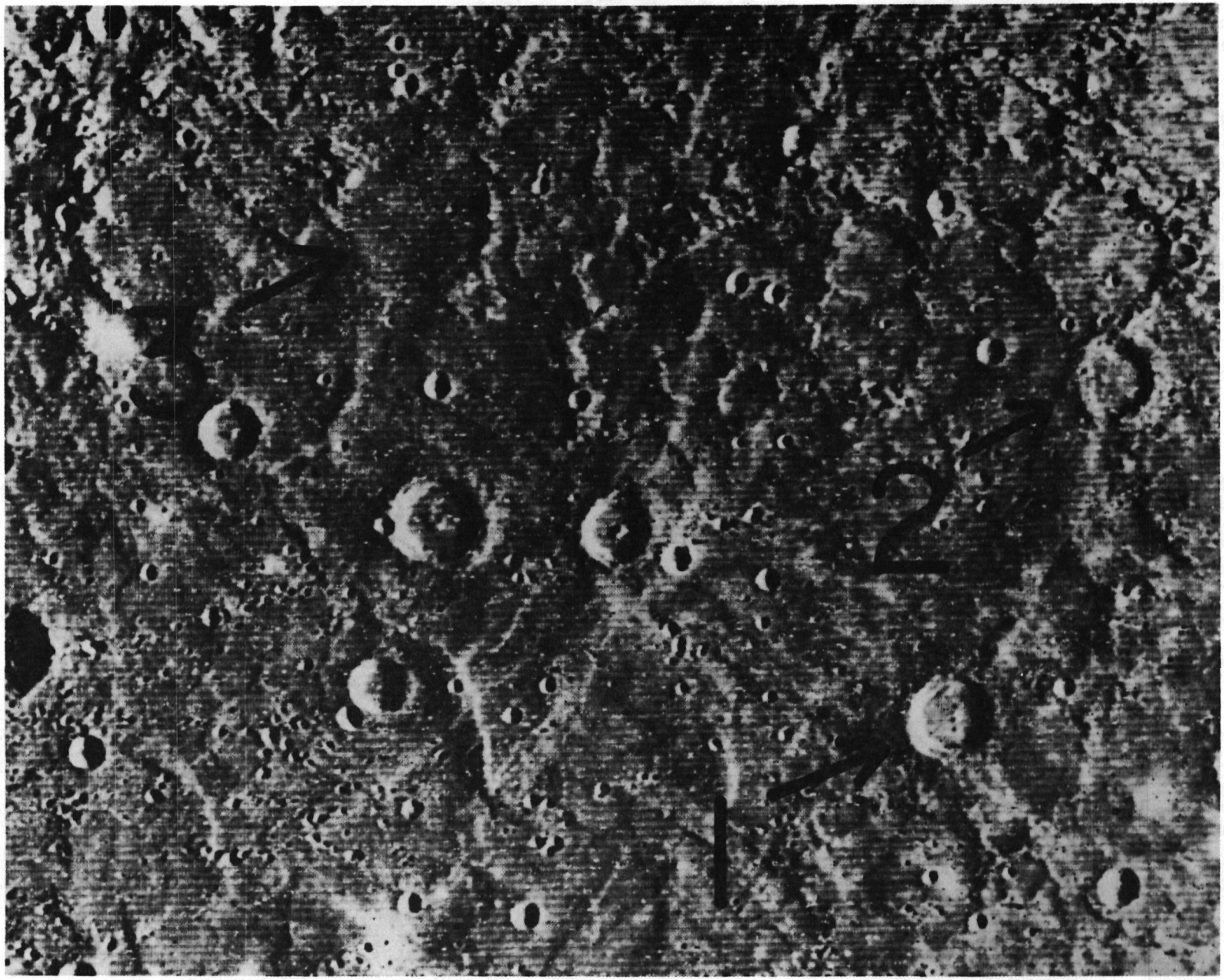

Figure 6.- Mercurian smooth plains illustrating class 1, 2, and 3 craters.

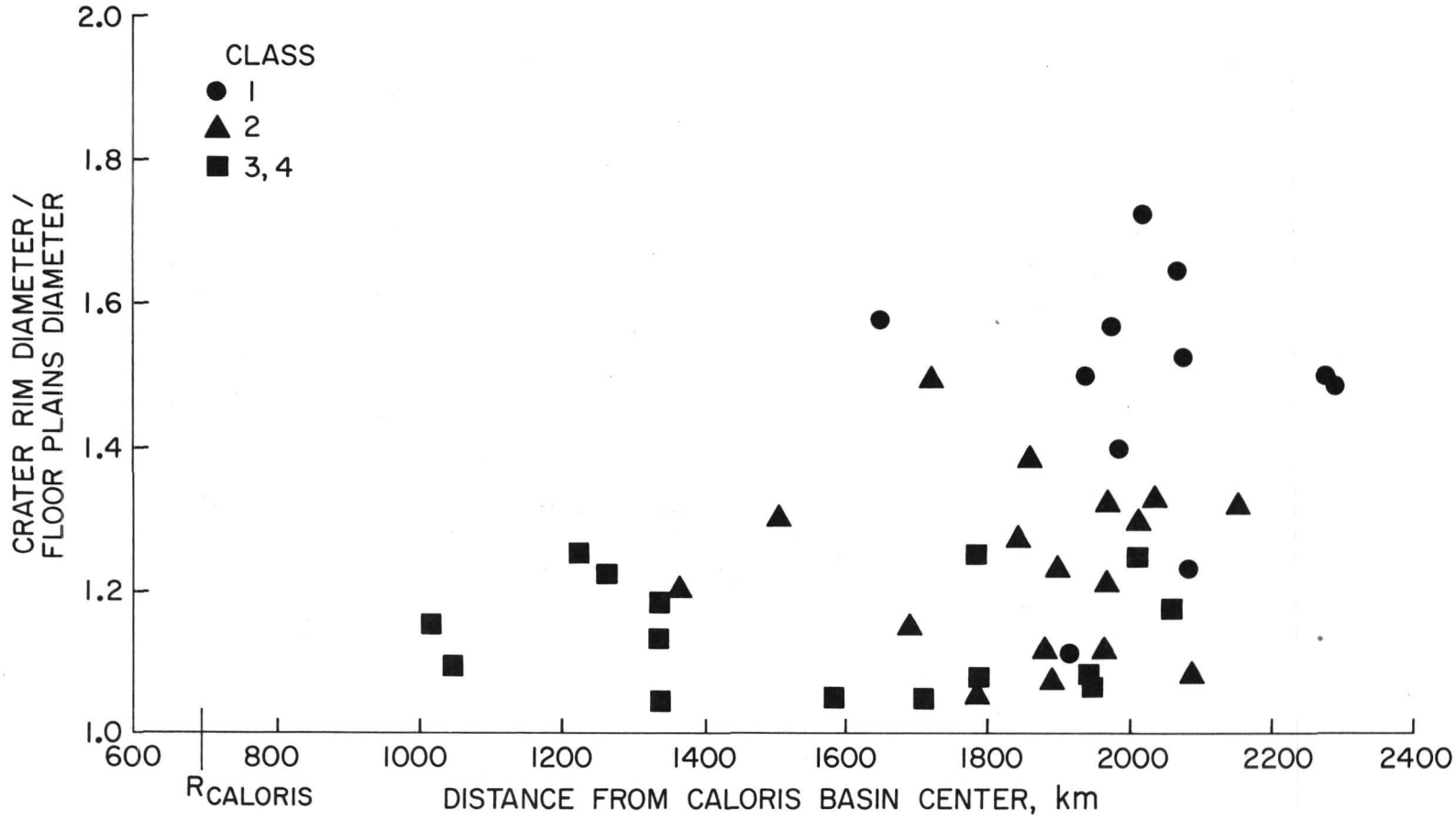

Figure 7.- Ratios of crater rim to floor diameters plotted as a function of range from the center of the Caloris basin. Symbols show crater class. The most degraded craters are nearest the basin and contain most of the plains.

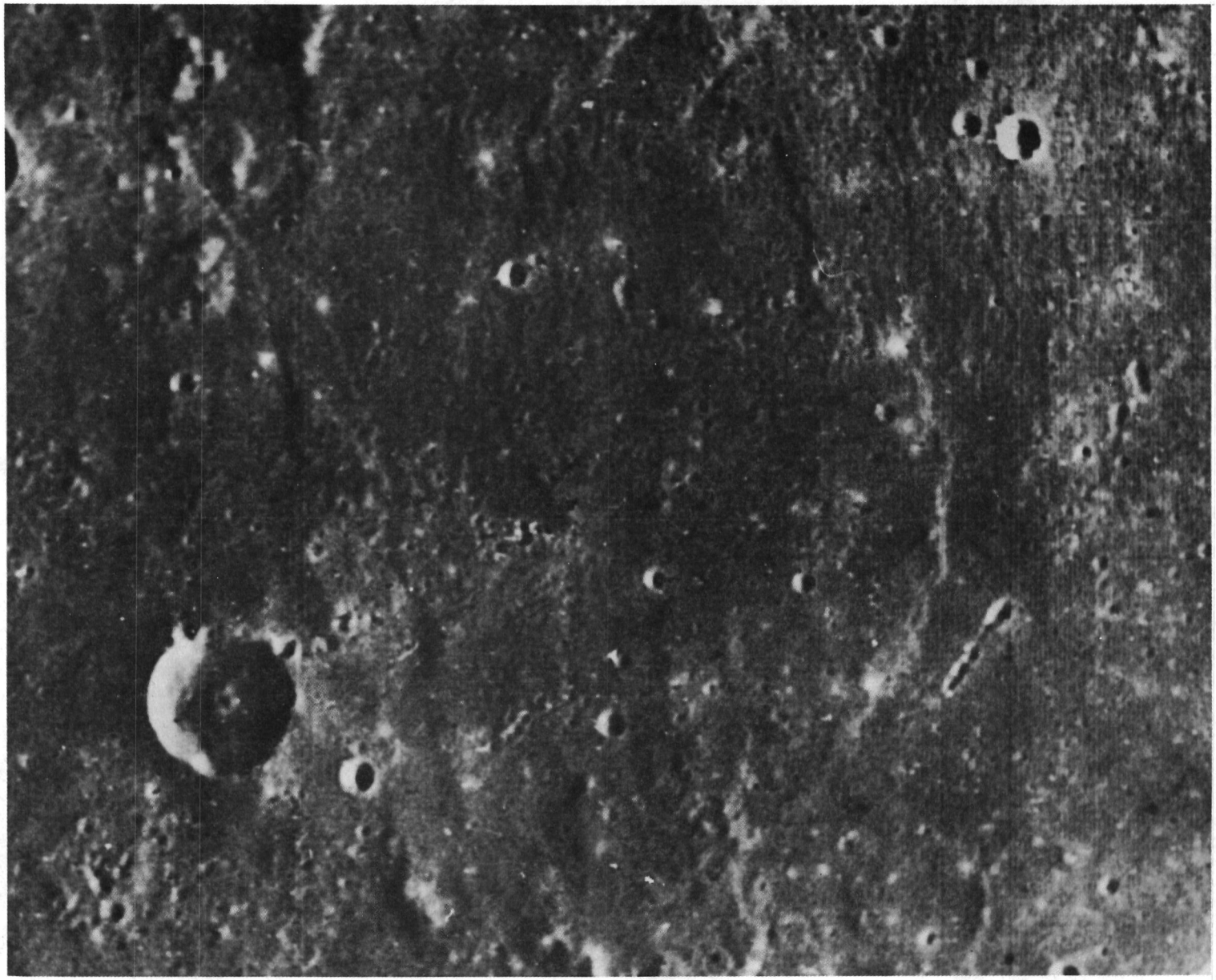

Figure 8. Hummocky facies of Caloris deposits can be seen to the upper right of this Mariner 10 frame of Mercurian smooth plains.

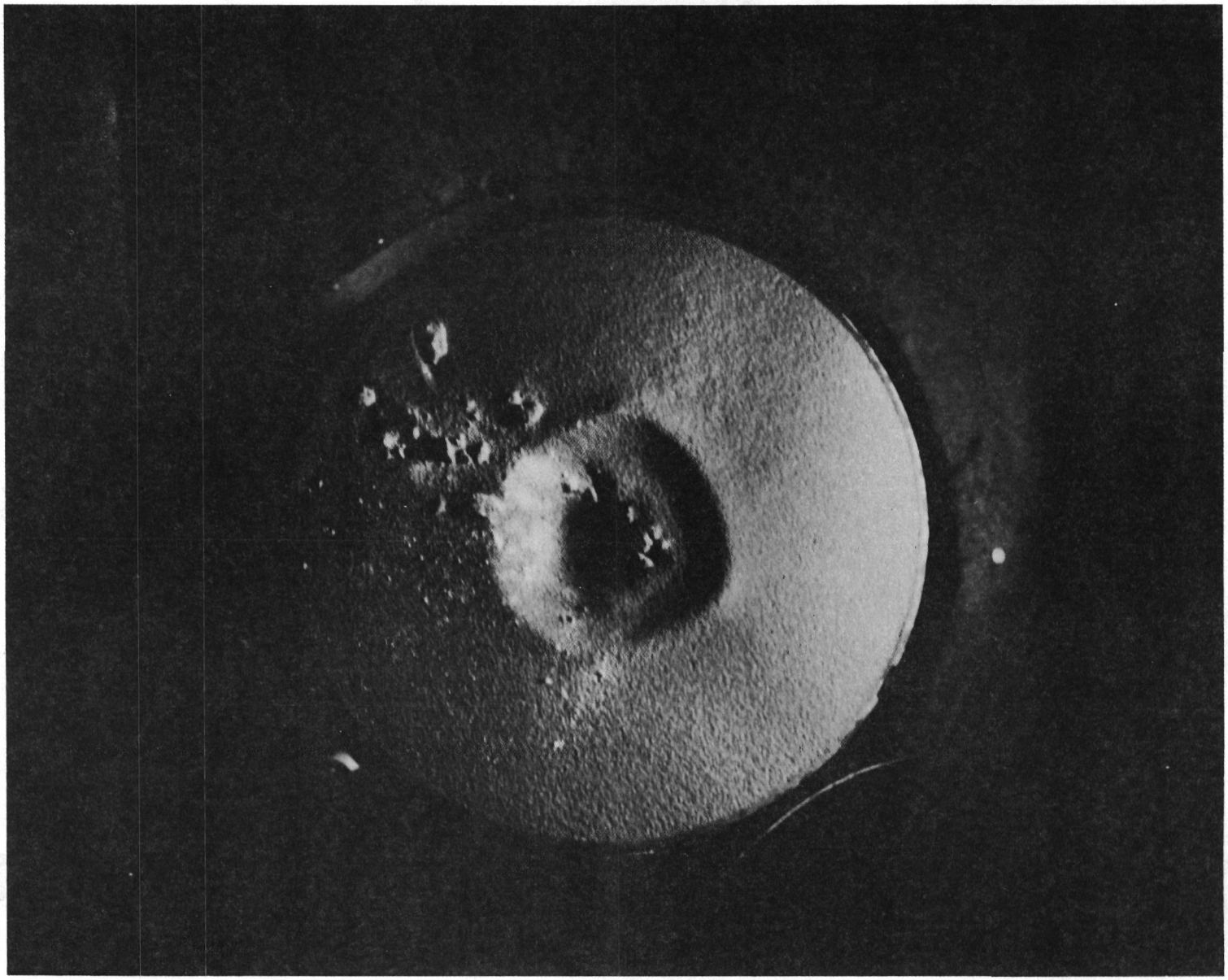

Figure 9.- Photograph of crater formed in layered target of sand resting on substrate of artificially cemented sandstone. Concentric crater is similar in geometry to the Ries crater.

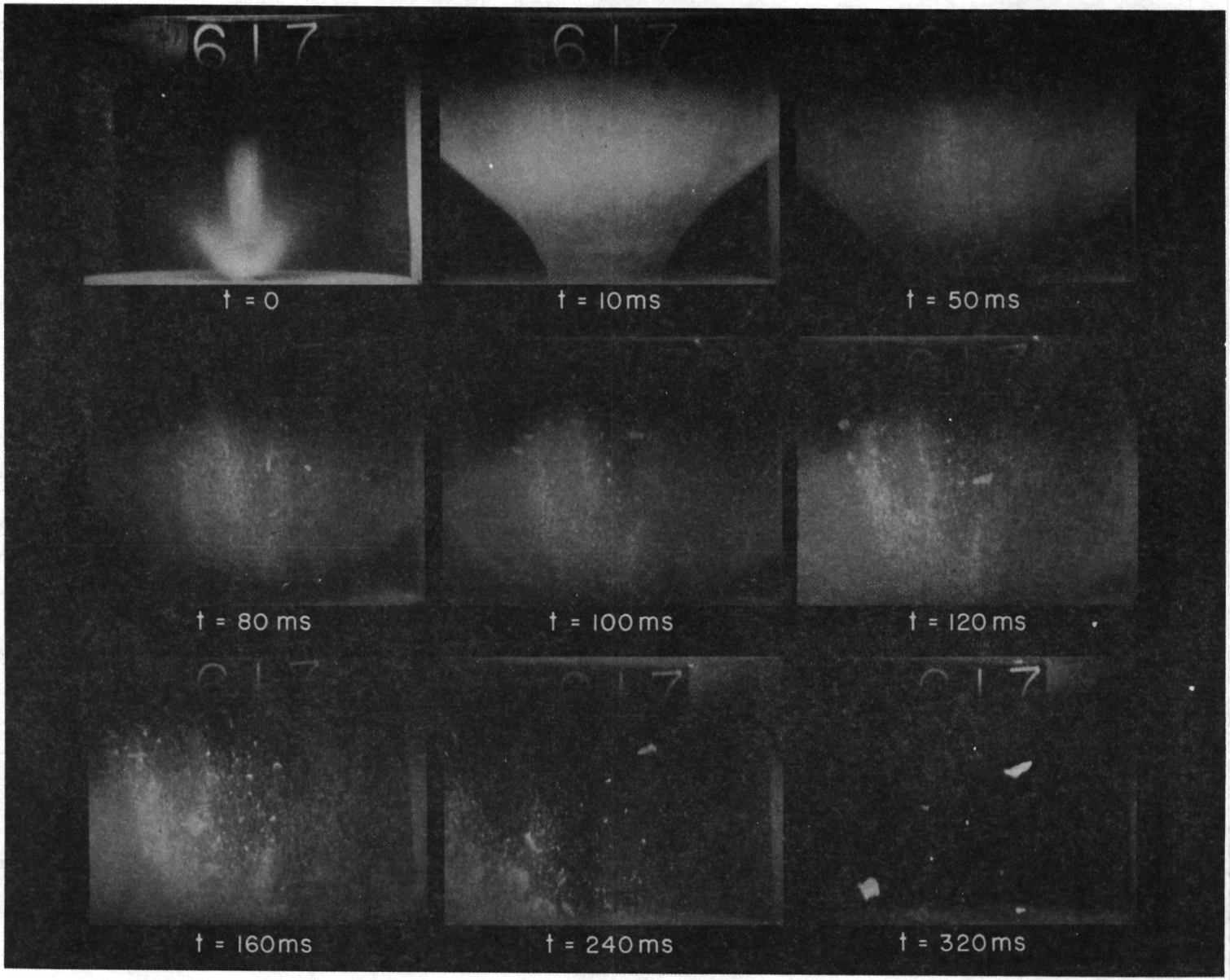

Figure 10.- High speed pictures of impact event that produced the crater shown in Figure 9. Note the near-vertical ejection of substrate material.

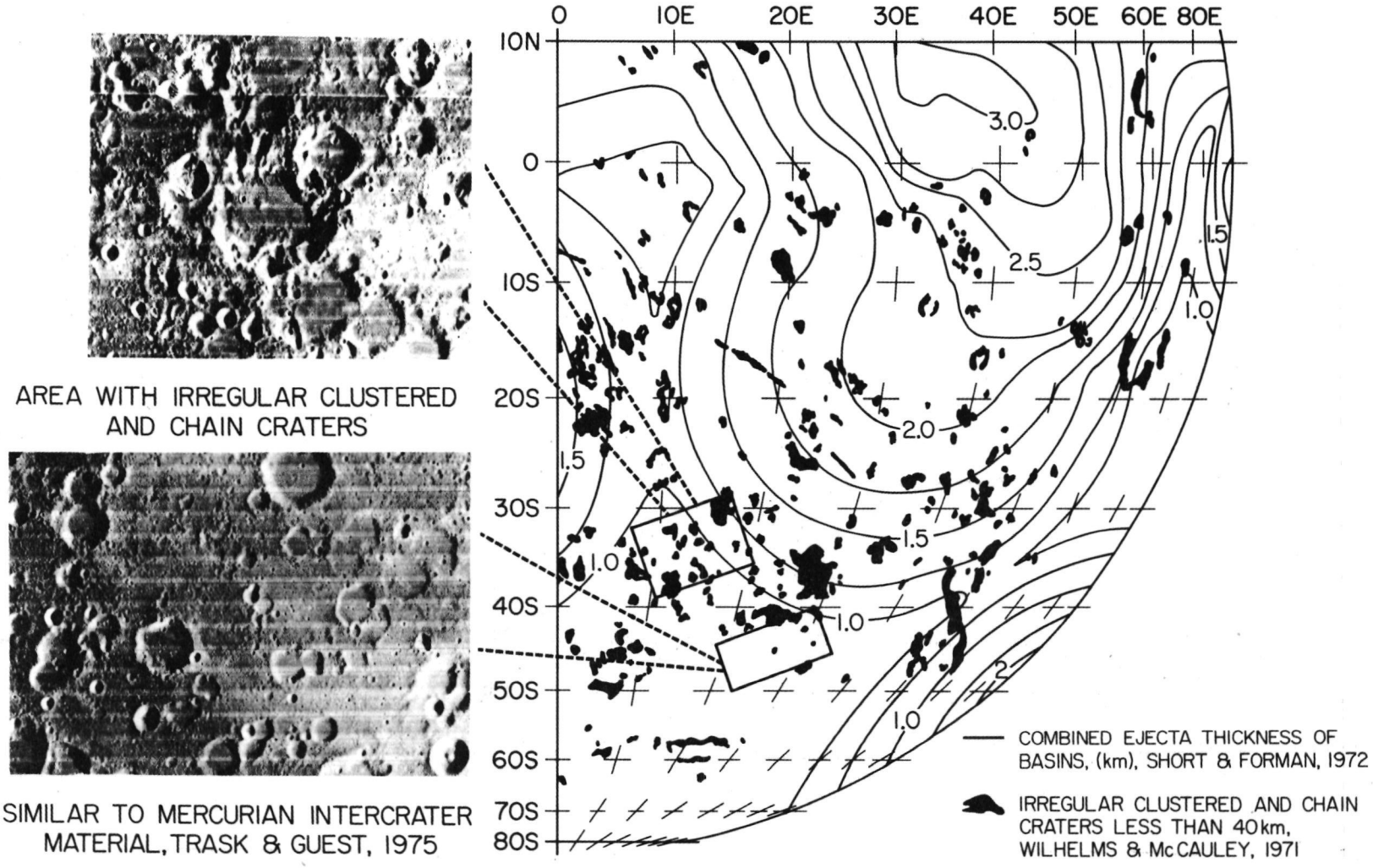

Figure 11.- Southeastern quadrant of the moon with a photograph of an area similar to Mercurian uplands, and a photograph of an area to the north containing large, irregular, chained, and clustered craters.

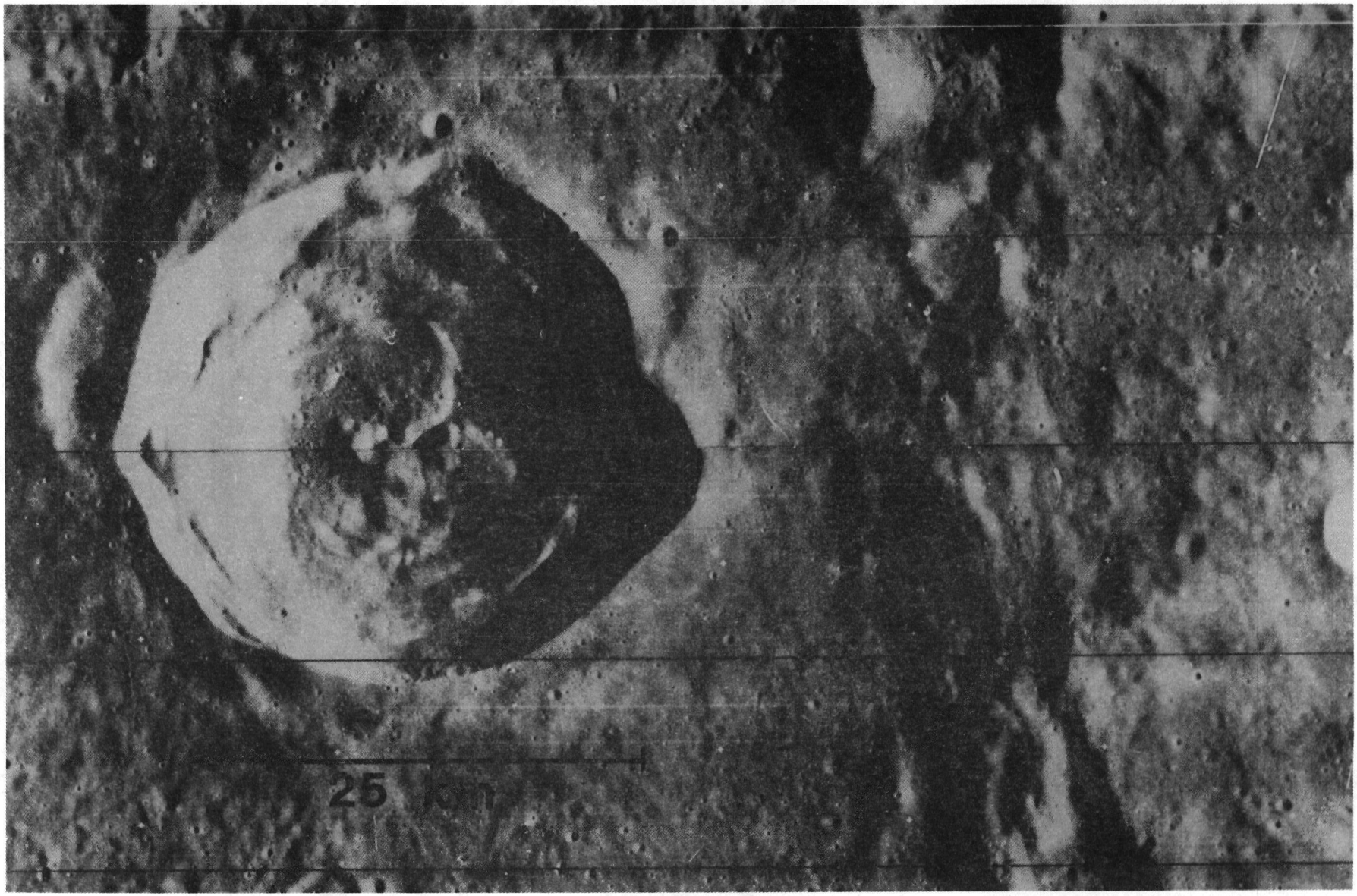

Figure 12.- Lunar crater Horrocks with septa and herringbone pattern suggestive of simultaneous secondary cratering events. Horrocks is ~30 km in diameter.

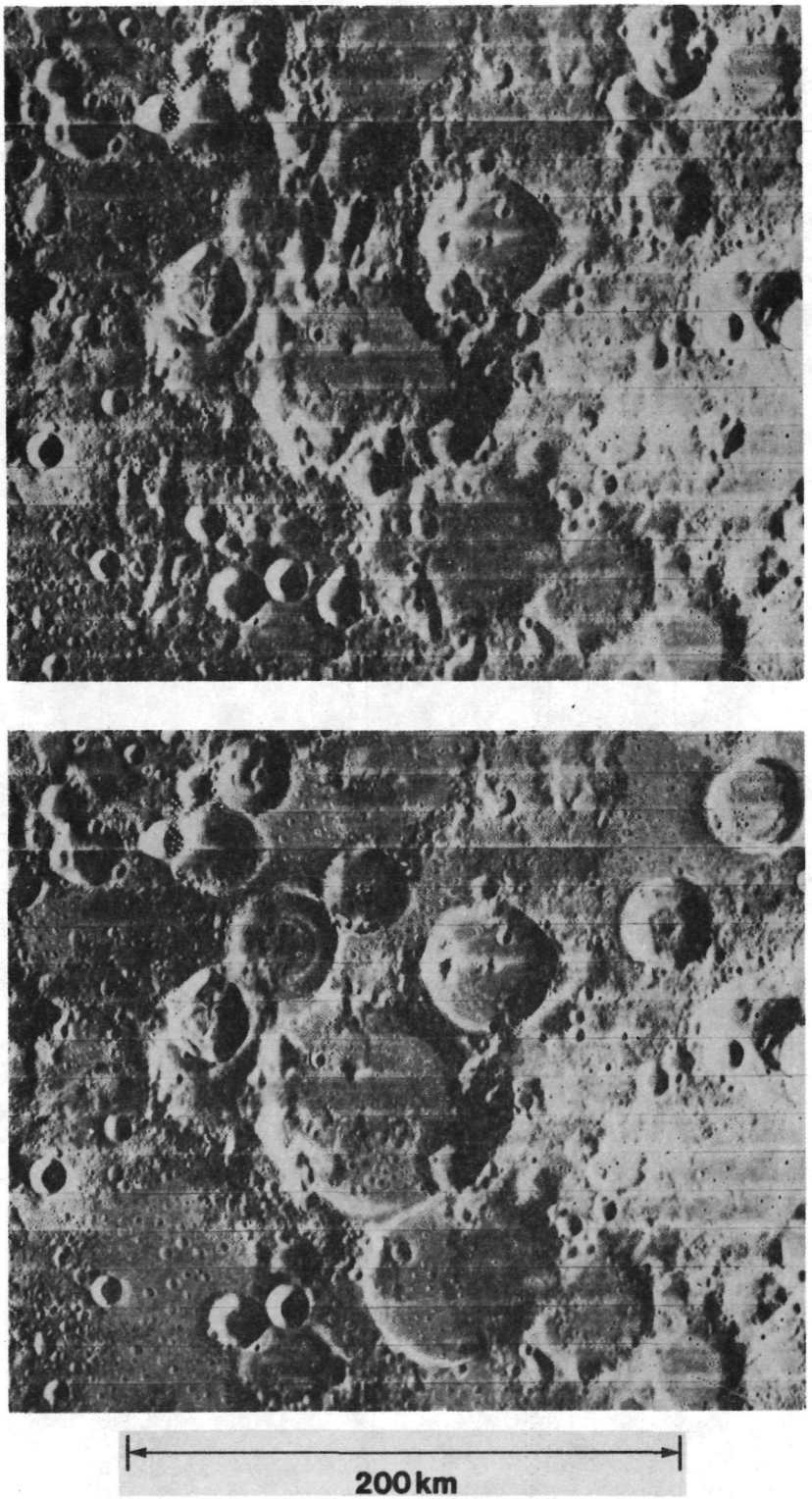

Figure 13.- The top photograph shows the area as in Figure 11 with the abundant irregular chained, and clustered craters. The lower photograph shows the same scene modified by airbrush removal of the irregular chained, and clustered craters mapped by Wilhelms and McCauley (1971). Rims have been airbrushed in where needed. The modified scene is similar to Mercurian uplands.

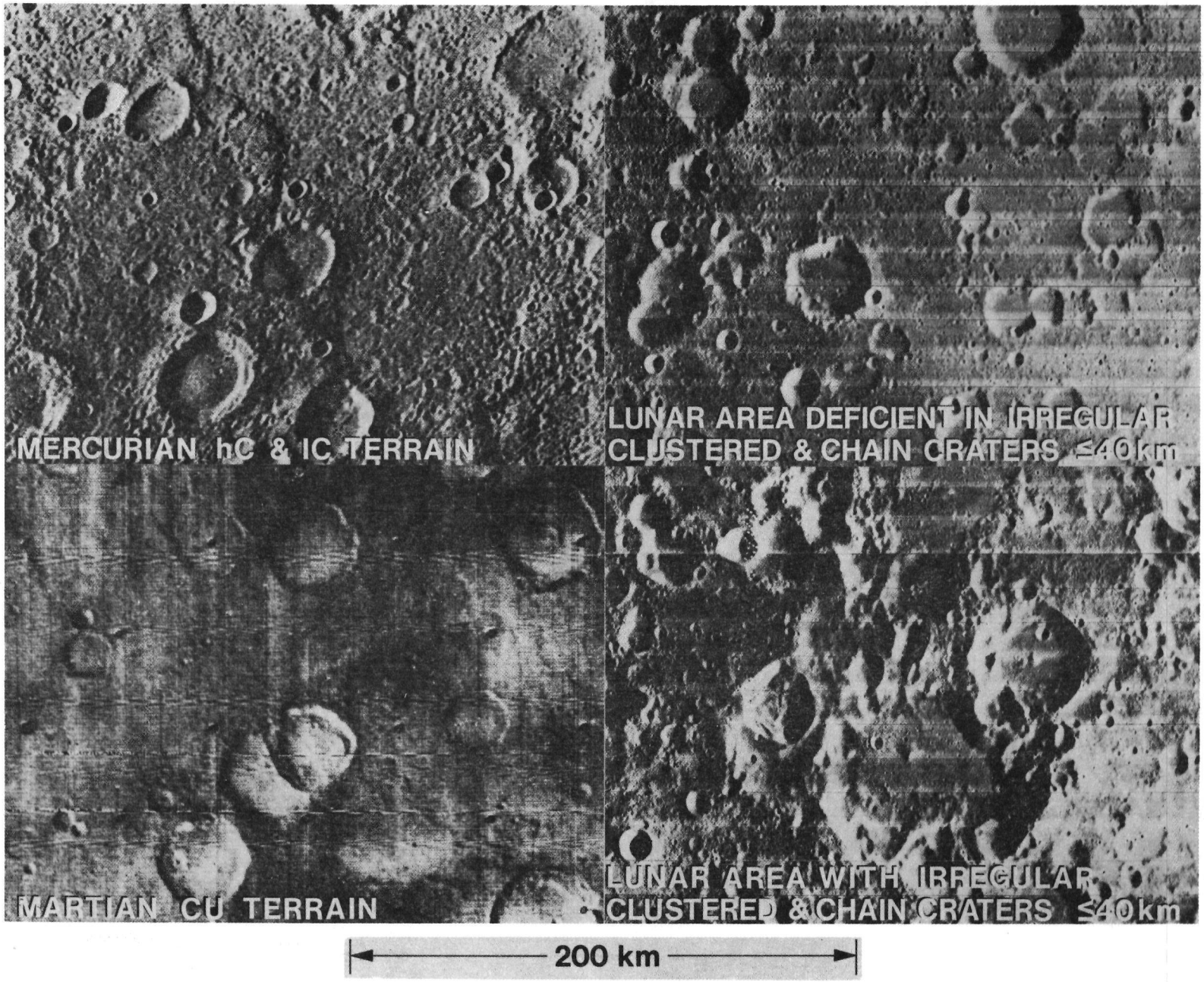

Figure 14.- Similar-sized scenes of the lunar, Martian, and Mercurian uplands.